PO Box 2345, Beijing 100023, China
www.wjgnet.com
wjg@wjgnet.com

World J Gastroenterol 2006 June 7; 12(21): 3359-3367
World Journal of Gastroenterology ISSN 1007-9327

BASIC RESEARCH

Effect of solanine on the membrane potential of mitochondria in HepG2 cells and $[Ca^{2+}]_i$ in the cells

Shi-Yong Gao, Qiu-Juan Wang, Yu-Bin Ji

Shi-Yong Gao, Qiu-Juan Wang, Physiology Section, Department of Pharmacy, China Pharmaceutical University, Nanjing, 210009, Jiangsu Province, China
Yu-Bin Ji, Postdoctoral Research Station, The Institute of Materia Medica, Harbin University of Commerce, Harbin 150076, Heilongjiang Province, China
Supported by the National Natural Science Foundation of China, No. 30400591; the Heilongjiang Province Natural Science Foundation, No. D2004-13, D200505; Harbin City Young Scientist Foundation, No. 2004AFQXJ035
Correspondence to: Professor Qiu-Juan Wang, Physiology Section, Department of Pharmacy, China Pharmaceutical University, 24 Tongjiaxiang Lane, Nanjing 210009, Jiangsu Province, China. wangqiujuan2005@sina.com
Telephone: +86-25-83271341
Received: 2005-11-29 Accepted: 2006-01-14

Abstract

AIM: To observe the effect of solanine on the membrane potential of mitochondria in HepG2 cells and $[Ca^{2+}]_i$ in the cells, and to uncover the mechanism by which solanine induces apoptosis.

METHODS: HepG2 cells were double stained with AO/EB, and morphological changes of the cells were observed using laser confocal scanning microscopy (LCSM). HepG2 cells were stained with TMRE, and change in the membrane potential of mitochondria in the cells were observed using LCSM. HepG2 cells were double stained with Fluo-3/AM, and change of $[Ca^{2+}]_i$ in the cells were observed using LCSM. HepG2 cells were double stained with TMRE and Fluo-3/AM, and both the change in membrane potential of mitochondria and that of $[Ca^{2+}]_i$ in the cells were observed using LCSM.

RESULTS: Cells in treated groups showed typical signs of apoptosis. Staining with TMRE showed that solanine could lower membrane potential; staining with Fluo-3/AM showed that solanine could increase the concentration of Ca^{2+} in tumor cells; and those of double staining with TMRE and Fluo-3/AM showed that solanine could increase the concentration of Ca^{2+} in the cells at the same time as it lowered the membrane potential of mitochondria.

CONCLUSION: Solanine opens up the PT channels in the membrane by lowering the membrane potential, leading to Ca^{2+} being transported down its concentration gradient, which in turn leads to the rise of the concentration of Ca^{2+} in the cell, turning on the mechanism for apoptosis.

Key words: Solanine; Hepatocarcinomatic cell; Ca^{2+} in the cell; Membrane potential; Laser confocal scanning microscopy

Gao SY, Wang QJ, Ji YB. Effect of solanine on the membrane potential of mitochondria in HepG2 cells and $[Ca^{2+}]_i$ in the cells. *World J Gastroenterol* 2006; 12(21): 3359-3367

http://www.wjgnet.com/1007-9327/12/3359.asp

INTRODUCTION

Solanine is found mainly in the tuber of the potato (Solanum tuberosum L.)[1-5] and in the whole plant of the nightshade (Solanum nigrum Linn) of the family Solanaceae. The content of this substance is rather high in the green peel and the sprouts of potato and is the main toxic substance[6]. The whole plant of the nightshade contains many steroid alkaloids, including solamargine, solasonine, and solanine, as well as saponin and other substances. It can be used for anti-tumor purposes, with a strong inhibitory effect on tumors in animals and a clearly toxic effect on tumor cells[7]. Its ethanol extract is capable of inhibiting the growth of breast cancer and induce apoptosis in tumor cells[8]. The extract from the nightshade also has a strong anti-inflammatory effect because it can facilitate the formation of antibodies[9]. The anti-tumor effect of solamargine has been reported[10], but there is as yet no report about any anti-tumor effect of solanine. From our past experience in both in vivo and in vitro experiments, we have found that solanine is cytotoxic to cells, especially for the hepatocarcinomatic cell HepG2. Through morphological observation, as well as DNA ladder and flow cytometry, we discovered that solanine exerted its anti-tumor effect by inducing apoptosis in HepG2.

The concept "apoptosis" was officially proposed by Kerr in 1972[11]. In the three decades since it was proposed, it has always been the focus of biological researches. Especially since 1990s, the study of apoptosis has suddenly been propelled to the frontier of life science, leading to an upsurge of research activities involving almost all the fields of biomedical studies. As a result, a great deal of literature accumulated in a few years about the

morphological characteristics of apoptosis, biochemical changes in apoptotic cells, genes regulating apoptosis, and various factors that can lead to apoptosis, as well as the relationship between apoptosis and health conditions. Membrane potential of mitochondria[12,13] and $[Ca^{2+}]_i$ in the cells[14,15], two factors closely associated with apoptosis, are themselves supplementary to and closely related with each other.

Rapid and continuous increase in the concentration of calcium ion is the earliest detectable biochemical change in cells undergoing apoptosis. The fact that the use of calcium-free culture medium and other methods capable of inhibiting the rise in the concentration of Ca^{2+} in cells can help to inhibit apoptosis[16] also shows that the rise in the concentration of Ca^{2+} in cells is an important condition for apoptosis to take place. A typical sign of apoptosis is the appearance of apoptotic bodies, but it is only when the concentration of Ca^{2+} has been raised that endogenous nuclease is activated, cutting the DNA chain between nucleosomes into discontinuous fragments (or apoptotic bodies), the basic unit of which is 180-200 bp long.

The mitochondrion is the storehouse for calcium in the cell, and change in its membrane potential can lead to Ca^{2+} and other ions being released from the mitochondrion or flowing into it, and the release and influx of Ca^{2+} and other ions are also the direct causes for changes in the membrane potential of mitochondrion. The essence of membrane potential change is the opening of the PT channels in the membrane. The opening of these channels precedes the release of Ca^{2+}, which is followed by changes in the membrane potential.

There are many approaches to studying apoptosis. In the present study, we tried to explicate the mechanism by which solanine induced apoptosis of tumor cells by focusing on the mitochondria and by observing the effect of solanine on the membrane potential of $HepG_2$ and $[Ca^{2+}]_i$ in the cell(Figure 1).

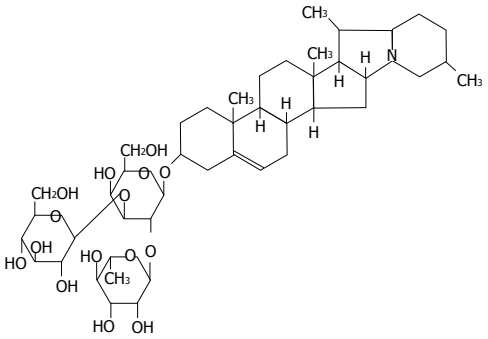

Figure 1 Molecular structure of solanine.

MATERIALS AND METHODS

Materials

The cell line: $HepG_2$ human hepatocarcinomatic cell lines were purchased from the Institute for Cancer Research, Heilongjiang Cancer Hospital.

Test drugs: Solanine with a purity of 99% was provided by Heilongjiang Institute For Drug Control.

Chemical reagents: RPMI 1640 culture medium was supplied from HyClone Laboratories; fetal bovine serum from Hangzhou Sijiqing Biological Engineering Materials Co.,Ltd; pancreatin from Gibio; ethidium bromide (EB) from AMRESCO; acridine orange (AO) from AMRESCO; Fluo-3/AM from Biotium, US; TMRE(molecular probe) from Biotium, US; HEPES from AMRESCO.

Preparation of the reagents: Fluo-3/AM 0.1 mg/stick was diluted to suitable concentration with DMSO, and then separately loaded and stored in the dark. TMRE 25 mg/stick was made into 1 mg/mL mother solution using anhydrous alcohol, separately loaded and stored in the dark. These were diluted with buffer solution for laboratory use and added to achieve the needed final concentrations before they were used in experiments.

Apparatuses: CO_2 incubator (CO-150, NBS, US); inverted microscope (CKX-41-32, Olympus, Japan); superclean bench (SW-CJ-2F, Suzhou Purification Equipments of the Sujing Group, Suzhou); laser confocal scanning microscope (SP2, Leica, Germany) were used.

Methods

Cell culture and treatment: $HepG_2$ cell culture was incubated in RPMI 1640 medium containing 10% fetal bovine serum at 50 mL/L CO_2 and 37℃, and transfer of culture was performed once every 3-4 d. When the cells grew steadily in the phase of logarithmic growth, 0.25% pancreatin was used to digest the cells. Digested cells were re-suspended using RPMI 1640 medium containing 10% fetal bovine serum and counted, and the concentration of cells was adjusted to 1×10^4 /mL. Cell suspension was added to the round troughs of 35 mm Petri dishes at 200 μL/dish, and the dishes were divided into 2, 0.4, 0.08, 0.016, and 0.0032 μg/mL treatment groups, the control, and the positive control (to be treated with camptothecine). After being incubated for 24 h at 50 mL/L CO_2 and 37℃, the treatment groups were treated with solanine of different concentrations so that their final concentrations were 2, 0.4, 0.08, 0.016, and 0.0032 μg/mL, respectively; an equal volume of RPMI 1640 was added to the control, while the positive control was treated with camptothecine, with a final concentration of 0.08 μg/mL. The dishes were then incubated for another 48 h at 50 mL/L CO_2 and 37℃ in CO_2 incubator.

Observation of Solanine-induced morphological changes of $HepG_2$ nuclei using LCSM: After 48 h, the cells were taken out of the incubator. The culture solution in the Petri dishes was sucked out, and the cells were rinsed 3 times with PBS at 5 min/time, double stained with 200 μL of acridine orange (AO)/ethidium brumide (EB) so that the final concentration was 5 μg/mL, incubated for 5-10 min at 37℃, and rinsed 3 times with PBS, 5 min/time. Then 200 μL of PBS was added, and LCSM was used to observe the morphology of the cells. Dual-channel activation was used, with an excitation wavelength of 488 nm and emission wavelength of 500-520 nm for PMT1(AO) and an excitation wavelength of 543 nm and emission wavelength of 600-700 nm for PMT2(EB)[17]. Other devices included Objective APO CS40 × /1.25 oil, zoom > 1, pinhole 1.5 Airy, mode XYZ, format 512 × 512.

Observation of Solanine-induced change in $[Ca^{2+}]_i$

in HepG2 cells using LCSM: After 48 h, the cells were taken out of the incubator. The culture solution in the Petri dishes was sucked out, and the cells were rinsed 3 times with HEPES, and 4 μg/mL Fluo-3/AM (Molecular Probes) was added, 200 μL/dish. After the cells were incubated at 37℃ for 50 min and rinsed with HEPES for 3 times, 200 μL of HEPES culture medium was used to cover all the cells in the troughs, and then LCSM was used to observe the fluorescence intensity (FI) of the cells, with an excitation wavelength of 488 nm and emission wavelength of 555 ± 15 nm. Other devices included objective APO CS40 ×/1.25 oil, zoom > 1, pinhole 1.5 Airy, mode XYZ, format 512 × 512.

Observation of Solanine-induced change in the membrane potential of the mitochondria in the cells using LCSM: After 48 h, the cells were taken out of the incubator. The culture solution in the Petri dishes was sucked out, the cells were rinsed 2-3 times with PBS, and 200 μL of tetramethyl rhodamine ethyl ester (TMRE, Molecular Probes) was gently added to the dishes, so that the final concentration was 2 μmol/L (1.03 μg/mL). The cells were then incubated for 30 min and, after the staining solution was sucked out, gently rinsed 3 times with PBS. 200 μL PBS was used to cover all the cells in the troughs, and then LCSM was used to observe the fluorescence intensity of the cells, with an excitation wavelength of 543 nm and emission wavelength of 570 ± 20 nm. Other devices included objective APO CS40 ×/1.25 oil, zoom > 1, pinhole 1.5 Airy, mode XYZ, format 512 × 512.

Simultaneous observation of changes in the morphology of cells, membrane potential, and the concentration of calcium in the cells: Experiment was performed on 2 groups of HepG2 cells simultaneously. Cell incubation, treatment, and operation procedures were all the same as above, with the same amount of time and conditions for cell incubation. One group was marked with AO/EB and the effect of solanine on its HepG2 cells was observed using LCSM; while HepG2 cells in the other group were marked with TMRE and Fluo-3/AM, and changes in membrane potential of the mitochondria and $[Ca^{2+}]_i$ in the cells were observed using LCSM. Methods for AO/EB double staining and measurement were as before, while the procedures for double staining with Fluo-3/AM and TMRE and measurement are as follows: (1) Staining after 48 h, the cells were taken out of the incubator. The culture solution in the Petri dishes was sucked out, the cells were rinsed 3 times with RPMI1640, and 150 μL of tetramethyl rhodamine ethyl ester (TMRE, Molecular Probes) working fluid with a concentration of 2 μmol/L (1.03 μg/mL) was pipetted onto the dishes. The cells were then incubated for 30 min at 37℃, and after the staining solution was sucked out, rinsed 3 times with RPMI1640. Finally 150 μL of Fluo-3/AM (Molecular Probes) with a concentration of 4 μg/mL was added. The cells were then incubated for 50 min at 37℃ and rinsed 3 times with RPMI1640, and 200 μL of RPMI1640 was added to cover all the cells in the troughs, whereupon the Petri dishes were mounted for measurement. (2) Observation LCSM was used to examine the fluorescence intensity (FI) of the cells. Dual-wavelength excitation was used, with excitation wavelengths of 488 nm and 543 nm, respectively. The emission wavelength used for PMT1 was 555 ± 15 nm, while that for PMT2 was 570 ± 20 nm. Other devices included Objective APO CS40 × /1.25 oil, zoom > 1, pinhole 1.5 Airy, mode XYZ, format 512 × 512. Sequential scanning was used to eliminate interference due to spectral overlap.

Statistical analysis

t test was performed on data obtained from the experiments, with the results expressed in the format mean ± SD. $P < 0.05$ was taken as significant.

RESULTS

Effect of Solanine on the morphology of HepG2 cells

After the DNA-specific fluorochromes AO and EB were used to stain HepG2 cells, LCSM was used to observe the morphological changes of HepG2 cells treated with solanine. From Figure 2A, it can be seen that the control was morphologically normal. The nuclei of different cells were of similar sizes, regularly shaped, and evenly stained. The more deeply colored parts of the nuclei represented heterochromatin which did not take part in transcription under normal circumstances. With solanine treatment, however, the cells showed marked morphological changes. In the groups treated with 0.0032 μg/mL and 0.016 μg/mL of solanine (Figures 2B and 2C, respectively), the cells were wrinkled, and the chromatin was concentrated and marginalized. In the group treated with 0.08 μg/mL of solanine (Figure 2D), cells with fragments and apoptotic bodies appeared, a typical sign for apoptosis. In the groups treated with 0.4 μg/mL and 2 μg/mL of solanine (Figures 2E and 2F, respectively), the number of cells containing apoptotic bodies was significantly increased. At the same time, it could be seen that high dosage of solanine was lethal to tumor cells, because with increasing dosage, the number of viable cells decreased significantly. Apoptotic bodies also appeared clearly in the positive control treated with camptothecin with the final concentration of 0.08 μg/mL.

Change induced by Solanine in $[Ca^{2+}]_i$ in HepG2 cells in the process of apoptosis

As shown in Figure 3 the effect of different dosages of solanine (0.0032, 0.016, 0.08, 0.4, and 2 μg/mL) on $[Ca^{2+}]_i$ in HepG2 cells was observed using LCSM with staining with the fluorescent probe Fluo-3/AM. On the left side of each group is the photograph (green) showing $[Ca^{2+}]_i$ taken under the confocal microscope, with the depth of the color representing the fluorescence intensity (FI). On the right is the 3D configuration reconstructed using LCSM for the group, with different colors reflecting different FI values, which indirectly reflect the concentrations of $[Ca^{2+}]_i$ for the test group in question. It is shown from these photographs that the $[Ca^{2+}]_i$ for the control in Figure 3A was very low, while those for the groups treated with solanine (Figures 3B-F) were all increased, in a concentration dependent manner. The positive control camptothecin did not increase $[Ca^{2+}]_i$. Statistics on FI obtained through LCSM for the various groups in Table 1 showed the same results.

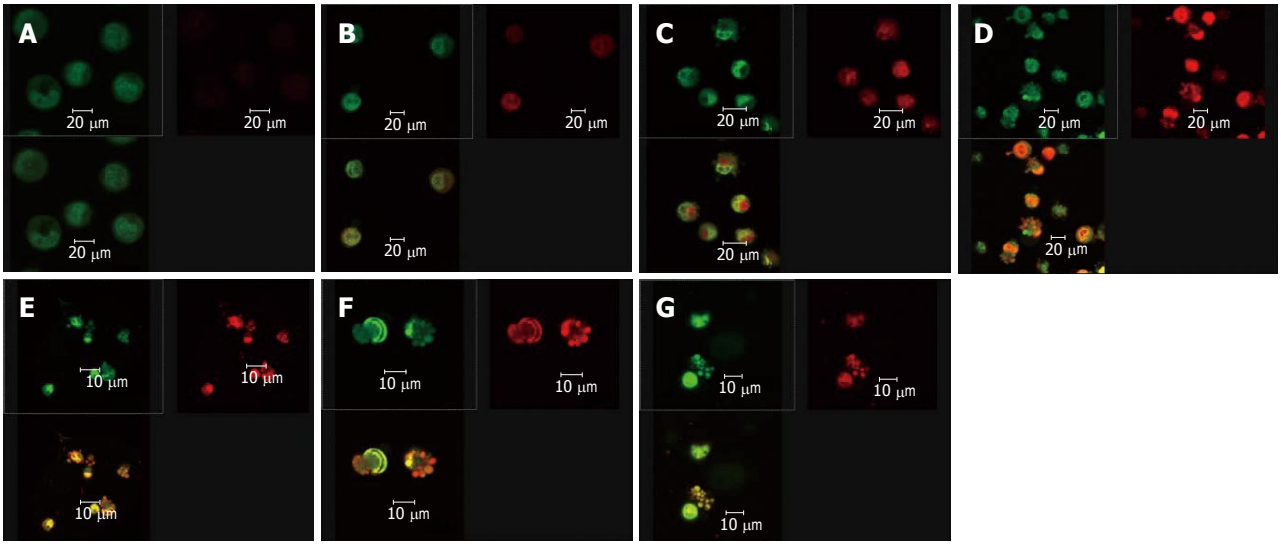

Figure 2 Effect of solanine on the morphology of HepG2. **A**: Control group, PMT1 nuclear chromatin was stained green and showed normal structure, while PMT2 showed no or only weak red fluorescence; **B**: Group treated with Solanine with final concentration of 0.0032 μg/mL: The cells show slightly pyknotic and crumb-shaped structures. Permeability of cell membrane has increased, so that AO and EB can enter the cells, resulting in the cells showing both green and red fluorescence; **C**: Group treated with Solanine with final concentration of 0.016 μg/mL: The cells show slightly pyknotic and crumb-shaped structure. Fragments or apoptotic bodies appear in the nuclei of some of the cells; **D**: Group treated with solanine with final concentration of 0.08 μg/mL: Cell structure is further damaged. The cells are not only stained with AO and EB, but morphologically the nuclei have become deeply stained fragments or apoptotic bodies; **E**: Group treated with solanine with final concentration of 0.4 μg/mL: Cell structure is damaged even further. Apoptotic bodies have definitely appeared; **F**: Group treated with solanine with final concentration of 2 μg/mL: Definite apoptotic bodies can be seen, while the number of cells in sight has decreased; **G**: Group treated with camptothecin with final concentration of 2 μg/mL: The appearance of apoptotic bodies is obvious in HepG2 cells.

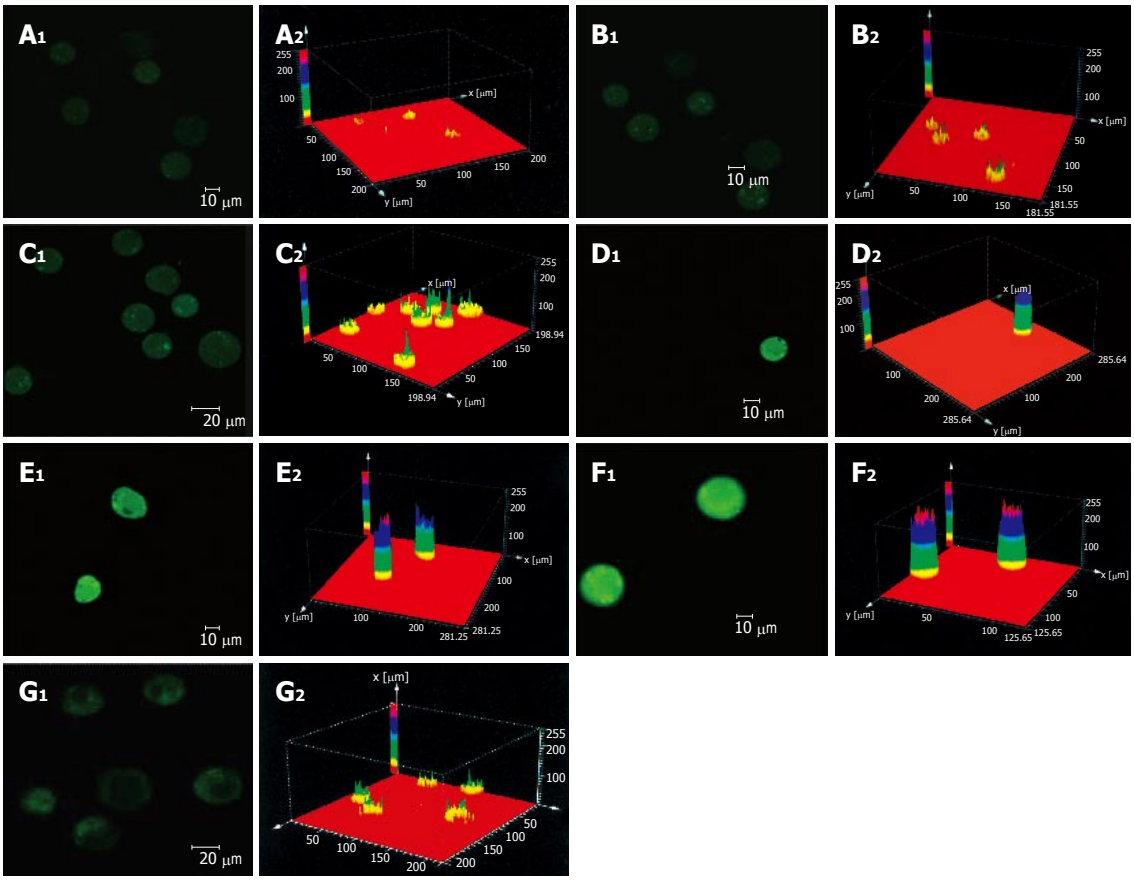

Figure 3 Effect of Solanine on $[Ca^{2+}]_i$ in HepG2 cells. **A**: Control; **B**: 0.0032 μg/mL solanine; **C**: 0.016 μg/mL solanine; **D**: 0.08 μg/mL solanine; **E**: 0.4 μg/mL solanine; **F**: 2 μg/mL solanine; **G**: 0.08 μg/mL camptothecin.

Change induced by Solanine in the membrane potential of mitochondria in HepG2 cells in the process of apoptosis

The effect of different dosages of solanine (0.0032, 0.016, 0.08, 0.4, and 2 μg/mL) on the membrane potential of mitochondria in HepG2 cells was observed using LCSM with staining by the fluorescent probe TMRE (Figure 4). The brightness of the coloration reflected different values of FI, thus indirectly indicating the membrane potential of mitochondria in the cells for these different groups. From those photographs, it could be seen that the membrane

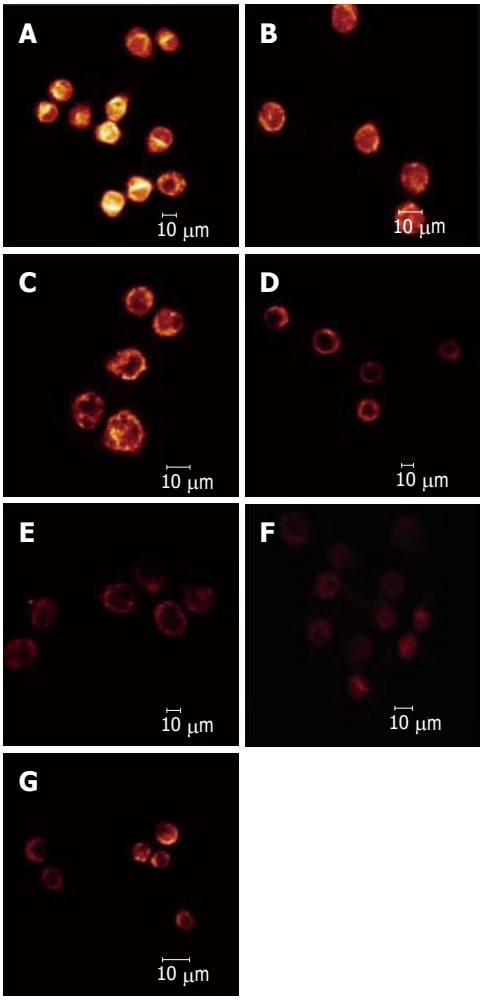

Figure 4 Effect of Solanine on membrane potential of mitochondria in $HepG_2$ cells. **A**: Control; **B**: 0.0032 μg/mL solanine; **C**: 0.016 μg/mL solanine; **D**: 0.08 μg/mL solanine; **E**: 0.4 μg/mL solanine; **F**: 2 μg/mL solanine; **G**: 0.08 μg/mL camptothecin.

Table 1 Effect of Solanine on $[Ca^{2+}]_i$ in $HepG_2$ cells (mean ± SD)

Group	Final concentration (μg/mL)	Number of cells (*n*)	FI
Control	-	18	23.98 ± 10.06
Camptothecin group	0.08	16	26.92 ± 8.20
Solanine groups	0.003	25	40.31 ± 10.15[b]
	0.016	37	59.31 ± 17.56[b]
	0.08	17	91.01 ± 23.19[b]
	0.4	19	158.75 ± 14.52[b]
	2	20	209.85 ± 10.86[b]

Comparison with blank: [b]$P < 0.01$.

Table 2 Effect of solanine on the membrane potential of mitochondria in $HepG_2$ cells (mean ± SD)

Group	Final concentration (μg/mL)	Cell number (*n*)	FI
Control	-	53	75.70 ± 31.24
Camptothecin group	0.08	16	47.17 ± 15.98
Solanine groups	0.003	66	70.04 ± 17.83
	0.016	90	63.21 ± 16.36[b]
	0.08	144	52.26 ± 26.46[b]
	0.4	37	32.50 ± 19.99[b]
	2	33	28.49 ± 9.71[b]

Comparison with blank: [b]$P < 0.01$.

potential of mitochondria in the cells was relatively high for the control in Figure 4A, while those for the groups treated with solanine (Figures 4B-F) were all increased, in a dosage dependent manner. Statistics on FI obtained through LCSM for the various groups in Table 2 showed that the membrane potential of mitochondria in the cells was significantly lowered ($P < 0.01$) in groups treated with 0.016, 0.08, 0.4, and 2 μg/mL of solanine. The membrane potential in the 0.0032 μg/mL group was also lowered, but the difference from the control was not significant. The membrane potential of mitochondria in $HepG_2$ cells of the group treated with 0.08 μg/mL of camptothecin was also significantly lowered.

Simultaneous observation of changes induced by solanine in cell morphology, $[Ca^{2+}]_i$ in cells, and mitochondrial membrane potential in $HepG_2$ cells in the process of apoptosis

Double staining with AO/BE and with Fluo-3/AM and TMRE were simultaneously used in this experiment (Figure 5). Changes in cell morphology, $[Ca^{2+}]_i$ in cells, and membrane potential of mitochondria in the same cell were simultaneously observed using LCSM for groups treated with different concentrations of solanine, so as to examine simultaneous changes in cell morphology, $[Ca^{2+}]_i$ in cells, and membrane potential of mitochondria in cells at the same time points in the apoptosis process induced by solanine of different concentrations and, moreover, to explore the physiological mechanisms of $[Ca^{2+}]_i$ and membrane potential of mitochondria in the cells and the relationship between them. As shown in Figure 5A for the control group, the cells were normal morphologically, and the $[Ca^{2+}]_i$ in the cells was relatively low, while the corresponding mitochondrial membrane potential was relatively high. Results for the groups treated with solanine (with final concentration of 0.0032, 0.016, 0.08, 0.4, and 2 μg/mL, respectively) are shown in Figures 5B-F. It could be seen that with the dosage increased, the shape of the cells gradually became more and more irregular, and typical apoptotic cells such as irregularly shaped cells and apoptotic bodies appeared, with apoptotic bodies, characteristic of apoptosis appearing first in the group treated with 0.08 μg/mL of solanine (Figure 5D). As the dosage increased, the percentage of apoptotic bodies gradually increased, and $[Ca^{2+}]_i$ in the cells also gradually increased, while the membrane potential of mitochondria in the cells gradually decreased for the corresponding groups. The group treated with camptothecin showed no change in $[Ca^{2+}]_i$ but it did show a significantly decreased membrane potential of mitochondria, results consistent with those obtained with single staining. It also showed that solanine induced apoptosis in $HepG_2$ cells by a

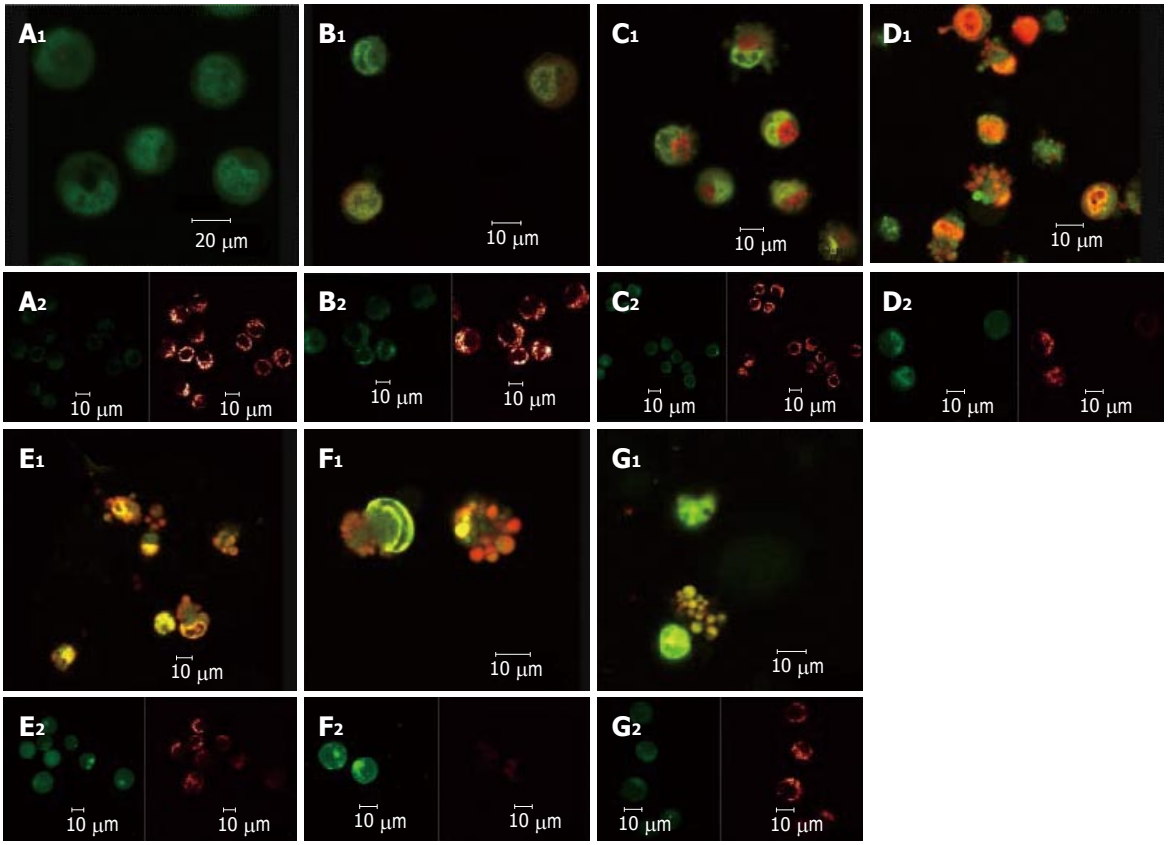

Figure 5 Changes induced by solanine in cell morphology, $[Ca^{2+}]_i$ in cells, and membrane potential of mitochondria in $HepG_2$ cells in the process of apoptosis. **A**: Control; **B**: 0.0032 μg/mL solanine; **C**: 0.016 μg/mL solanine; **D**: 0.08 μg/mL solanine; **E**: 0.4 μg/mL solanine; **F**: 2 μg/mL solanine; **G**: 0.08 μg/mL camptothecin.

Table 3 Effect of solanine on $[Ca^{2+}]_i$ in $HepG_2$ cells and mitochondrial membrane potential (mean ± SD)

Group	Final concentration (μg/mL)	Number of cells	Fluo-3/AM-FI	TMRE-FI
Control	-	111	24.96 ± 4.03	51.85 ± 19.18
Camptothecin group	0.08	21	28.80 ± 7.01	25.50 ± 5.76[b]
Solanine groups	0.003	49	33.85 ± 9.30[a]	39.52 ± 15.41[b]
	0.016	33	34.37 ± 14.18[a]	35.01 ± 11.12[c]
	0.08	36	42.73 ± 14.75[b]	28.13 ± 4.31[d]
	0.4	39	52.80 ± 11.07[b]	23.21 ± 12.22[d]
	2	37	58.62 ± 16.04[b]	13.09 ± 4.71[d]

Comparison with blank: [a]$P < 0.05$; [b]$P < 0.01$; [c]$P < 0.005$; [d]$P < 0.001$.

different mechanism from camptothecin. Detailed changes of different groups are shown in Table 3.

Solanine-induced changes in $[Ca^{2+}]_i$ and membrane potential of mitochondria in $HepG_2$ cells in the process of apoptosis and their distribution in the cells

When the images for the double staining with Fluo-3/AM and TMRE were recombined using the image analyzing capacity of the laser confocal scanning microscope, it could be seen that Ca^{2+} was widely distributed in the whole cell, but with different concentrations in different regions of the cell. In contrast, membrane potential of mitochondria was distributed only in certain parts of the cell (Figure 6). Superimposing the two images, it can be seen that regions where Ca^{2+} was more concentrated were basically also those where membrane potential was distributed.

DISCUSSION

The mitochondrion is an important organelle of the eukaryotic cell and the main site for the production of ATPs in animal cells[18,19]. NADH is produced from the tricarboxylic cyclophorase series in mitochondrial matrix through the dehydroxidization of the substrate, and then oxidized through the electron transport chain on the inner membrane of the mitochondrion. This leads to the transmembrane transfer of protons, resulting in a transmembrane proton gradient (or transmembrane potential). The ATP synthetase on the inner membrane of the mitochondrion synthesizes ATPs using the energy derived from the proton gradient. Through the ADP/ATP carriers on the inner membrane of mitochondria, ATPs synthesized this way are exchanged for ADPs from the cytoplasm, thus entering the cytoplasm to take part in various processes requiring energy.

In recent years, reports have been made that the dissipation of the membrane potential of mitochondria precedes the activation of nuclease[20], and that it precedes the exposure of phosphatidylserine on the surface of the cell. When the transmembrane potential of mitochondria is dissipated, the cell would enter the irreversible apoptotic process. The uncoupled respiratory chain of the mitochondrion would produce a large amount of active oxygen, oxidizing the cardiolipin on the inner membrane of the mitochondrion. Experiments have shown that the decoupling reagent mClCCP can lead to the apoptosis of

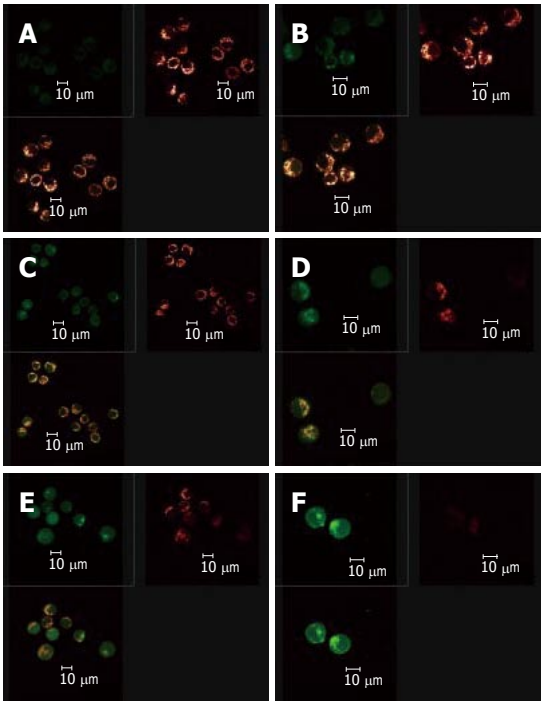

Figure 6 Distribution of solanine-induced changes in $[Ca^{2+}]_i$ and membrane potential of mitochondria in the $HepG_2$ cells in the process of apoptosis. **A**: Blank; **B**: 0.0032 μg/mL solanine; **C**: 0.016 μg/mL solanine; **D**: 0.08 μg/mL solanine; **E**: 0.4 μg/mL solanine; **F**: 2 μg/mL solanine.

lymphocytes[21,22], whereas if the transmembrane potential of mitochondria can be stabilized, apoptosis would be prevented. Therefore, the dissipation of transmembrane potential of mitochondria is closely related to apoptosis.

The dissipation of transmembrane potential of mitochondria in the process of apoptosis is mainly caused by changes in the permeability of the inner membrane of mitochondria, which is due to the formation of dynamic pores for permeability transition (PT) (each composed of several proteins) at points of contact between the outer and inner membranes of the mitochondrion[23]. PT channels are made up of proteins from various parts of the mitochondrion and those from the cytoplasm[24,25]. They include a protein in the cytochylema (hexokinase)[25], proteins on the outer membrane of the mitochondrion (peripheral benzodiazepine receptors and voltage-dependent anion channels), a protein in the interstice between the inner and outer membranes of the mitochondrion (creatine kinase)[26], a protein on the inner membrane of the mitochondrion (the ADP-ATP carrier)[27], and a protein in the mitochondrial matrix (cyclophilin D)[28]. Any substance, such as protoporphyria IX, the ligand for benzodiazepine receptors, that can specifically induce the formation of PT channels in mitochondria could cause apoptosis[29-32]. PT channels are a kind of channels with high electric conductivity. The lowering or even disappearance of membrane potential would suggest that PT channels are open.

Results from earlier experiments show that solanine can induce the apoptosis of $HepG_2$ cells. In the present study, double staining with AO/EB and solanine (0.0032, 0.016, 0.08, 0.4, and 2 μg/mL) carried by TMRE were used to treat $HepG_2$ cells, and LCSM was used to observe changes in the membrane potential of mitochondria as solanine induced the appearance of apoptotic bodies[33]. As solanine induced the appearance of apoptotic bodies and caused the apoptosis of cells, the membrane potentials of mitochondria in cells in groups treated with different dosages of solanine (0.0032, 0.016, 0.08, 0.4, and 2 μg/mL) were all decreased in comparison with the control (Figures 2 and 4, and Table 2). The amount of decrease was dosage-dependent, and the difference from that of the control was significant for the groups treated with 0.016, 0.08, 0.4, and 2 μg/mL of solanine, respectively, suggesting that solanine can lead to the lowering of the membrane potential of mitochondria in $HepG_2$ cells. However, the lowering of the membrane potential of mitochondria is a manifestation of the opening of the PT pores of the mitochondria[34], so solanine can lead to the opening of the PT pores of the mitochondria.

The opening of PT pores can lead to the occurrence of two events[35]: (1) the intra-membrane and extra-membrane ion concentrations tend toward equilibrium, the transmembrane H^+ gradient disappears, and the respiratory chain is uncoupled; (2) the flow of intra- and extra-membrane ions toward equilibrium leads to a hypertonic mitochondrial matrix, resulting in change in the volume of the mitochondrion. Since the surface area of the folded inner membrane of mitochondrion is larger than that of the outer membrane, this would lead to the rupture of the outer membrane.

These two events lead respectively to two consequences. Since a large number of Ca^{2+} have accumulated in mitochondria, the concentration of Ca^{2+} in mitochondria is much higher than that in the cytoplasm. The occurrence of the first event would lead directly to the flow of Ca^{2+} from the mitochondria to the cytoplasm, resulting in rapid increase in the concentration of Ca^{2+} in the cytoplasm. In the present study, the Ca^{2+}-specific molecular probe Fluo-3/AM was used to carry solanine at different concentrations to treat $HepG_2$ cells, and LCSM was used to observe changes in $[Ca^{2+}]_i$ in the cells after the treatment. In groups treated with different dosages of solanine (0.0032, 0.016, 0.08, 0.4, and 2 μg/mL), the concentrations of Ca^{2+} in $HepG_2$ cells were all increased in a dosage-dependent way (Figure 3 and Table 1). This verifies the inference we have drawn, namely, by opening up PT channels, solanine leads to the release of Ca^{2+} from the mitochondria, resulting in the increase of $[Ca^{2+}]_i$ in the cell. In order to obtain more powerful evidence for our inference, LCSM with double staining with Fluo-3/AM and TMRE was used to observe simultaneously the change in membrane potential and the change in $[Ca^{2+}]_i$ in the cell after the treatment. The results showed that as the dosage increased, the rate of apoptosis gradually increased, the membrane potential gradually decreased, and $[Ca^{2+}]_i$ in the cell gradually increased (Figure 5 and Table 3). These results were consistent with that obtained with single staining.

At the same time, the data collected using LCSM was analyzed and observation was made on the distribution of $[Ca^{2+}]_i$ and the membrane potential of mitochondria in the cells in the apoptotic process of $HepG_2$ induced by solanine. The image overlay function of LCSM was used

to superimpose and compare the images of $[Ca^{2+}]_i$ and the membrane potential of mitochondria in the cells. Results showed that membrane potential was mainly distributed on the inner membrane of the cells, with no distribution in the center of the cells; but the inner membrane was precisely where mitochondria were concentrated (Figure 6). $[Ca^{2+}]_i$ was distributed throughout the whole cell, but the distribution was uneven. This can be observed in the photograph with green fluorescence in Figure 6, where the brightness of the fluorescence depends on the region of the cell. When the image for $[Ca^{2+}]_i$ distribution (green) was superimposed on that for membrane potential (red), it can be seen that regions where Ca^{2+} was concentrated overlaps with where membrane potential was concentrated (as shown by the yellow regions in the third photograph in each group in Figure 6), suggesting that the distribution of Ca^{2+} in the mitochondria was high. In addition, the concentration of Ca^{2+} in both the mitochondria and the cytoplasm continued to rise in the different groups, suggesting that as $[Ca^{2+}]_i$ increased in the cytoplasm, Ca^{2+} flew out not only from the mitochondria, but also from some other source(s) as well, e.g., an inflow of Ca^{2+} from outside the cell.

In conclusion, solanine can facilitate the opening of the PT channels in mitochondria, leading to release of Ca^{2+} from these organelles. This results in an increase in the concentration of Ca^{2+} in the cell, thus triggering the mechanism for apoptosis and the occurrence of apoptosis. However, to uncover how the PT channels are opened and which enzymes and genes are involved in this process, further research is needed.

REFERENCES

1 **Kodamatani H**, Saito K, Niina N, Yamazaki S, Tanaka Y. Simple and sensitive method for determination of glycoalkaloids in potato tubers by high-performance liquid chromatography with chemiluminescence detection. *J Chromatogr A* 2005; **1100**: 26-31

2 **Shindo T**, Ushiyama H, Kan K, Yasuda K, Saito K. [Contents and its change during storage of alpha-solanine and alpha-chaconine in potatoes]. *Shokuhin Eiseigaku Zasshi* 2004; **45**: 277-282

3 **Zywicki B**, Catchpole G, Draper J, Fiehn O. Comparison of rapid liquid chromatography-electrospray ionization-tandem mass spectrometry methods for determination of glycoalkaloids in transgenic field-grown potatoes. *Anal Biochem* 2005; **336**: 178-186

4 **Wang S**, Panter KE, Gaffield W, Evans RC, Bunch TD. Effects of steroidal glycoalkaloids from potatoes (Solanum tuberosum) on in vitro bovine embryo development. *Anim Reprod Sci* 2005; **85**: 243-250

5 **Bodart P**, Noirfalise A. [Glycoalkaloids in potatoes]. *Rev Med Liege* 2003; **58**: 25-32

6 **Korpan YI**, Nazarenko EA, Skryshevskaya IV, Martelet C, Jaffrezic-Renault N, El'skaya AV. Potato glycoalkaloids: true safety or false sense of security? *Trends Biotechnol* 2004; **22**: 147-151

7 **Ji YB**. Pharmacological Action and Application of Available Composition of Traditional Chinese Medicine. 1st ed. Heilongjiang: Heilongjiang Science and Technology Press, 1995: 433

8 **Son YO**, Kim J, Lim JC, Chung Y, Chung GH, Lee JC. Ripe fruit of Solanum nigrum L. inhibits cell growth and induces apoptosis in MCF-7 cells. *Food Chem Toxicol* 2003; 41: 1421-1428

9 **Liu Chun-An**, Peng Ming. Dictionary of Anti-tumor Herb. 1st ed. Hubei: Hubei Sciences and Technology Press, 1994: 294-297

10 **Liu LF**, Liang CH, Shiu LY, Lin WL, Lin CC, Kuo KW. Action of solamargine on human lung cancer cells--enhancement of the susceptibility of cancer cells to TNFs. *FEBS Lett* 2004; **577**: 67-74

11 **Kerr JF**, Wyllie AH, Currie AR. Apoptosis: a basic biological phenomenon with wide-ranging implications in tissue kinetics. *Br J Cancer* 1972; **26**: 239-257

12 **Hwang JM**, Kuo HC, Tseng TH, Liu JY, Chu CY. Berberine induces apoptosis through a mitochondria/caspases pathway in human hepatoma cells. *Arch Toxicol* 2006; **80**: 62-73

13 **Lugli E**, Troiano L, Ferraresi R, Roat E, Prada N, Nasi M, Pinti M, Cooper EL, Cossarizza A. Characterization of cells with different mitochondrial membrane potential during apoptosis. *Cytometry A* 2005; **68**: 28-35

14 **Lépine S**, Sulpice JC, Giraud F. Signaling pathways involved in glucocorticoid-induced apoptosis of thymocytes. *Crit Rev Immunol* 2005; **25**: 263-288

15 **Pretorius E**, Bornman MS. Calcium-mediated aponecrosis plays a central role in the pathogenesis of estrogenic chemical-induced neurotoxicity. *Med Hypotheses* 2005; **65**: 893-904

16 **Palaga T**, Kataoka T, Woo JT, Nagai K. Suppression of apoptotic cell death of IL-3-dependent cell lines by ER/SR Ca2+-ATPase inhibitors upon IL-3 deprivation. *Exp Cell Res* 1996; **228**: 92-97

17 **Bernas T**, Asem EK, Robinson JP, Cook PR, Dobrucki JW. Confocal fluorescence imaging of photosensitized DNA denaturation in cell nuclei. *Photochem Photobiol* 2005; **81**: 960-969

18 **Brookes PS**, Yoon Y, Robotham JL, Anders MW, Sheu SS. Calcium, ATP, and ROS: a mitochondrial love-hate triangle. *Am J Physiol Cell Physiol* 2004; **287**: C817-C833

19 **Erecinska M**, Cherian S, Silver IA. Energy metabolism in mammalian brain during development. *Prog Neurobiol* 2004; **73**: 397-445

20 **Zhang M**, Li Y, Zhang H, Xue S. BAPTA blocks DNA fragmentation and chromatin condensation downstream of caspase-3 and DFF activation in HT-induced apoptosis in HL-60 cells. *Apoptosis* 2001; **6**: 291-297

21 **O'Brien KA**, Muscarella DE, Bloom SE. Differential induction of apoptosis and MAP kinase signaling by mitochondrial toxicants in drug-sensitive compared to drug-resistant B-lineage lymphoid cell lines. *Toxicol Appl Pharmacol* 2001; **174**: 245-256

22 **Duchen MR**. Contributions of mitochondria to animal physiology: from homeostatic sensor to calcium signalling and cell death. J Physiol 1999; **516**: 1-17

23 **Panov AV**, Lund S, Greenamyre JT. Ca^{2+}-induced permeability transition in human lymphoblastoid cell mitochondria from normal and Huntington's disease individuals. *Mol Cell Biochem* 2005; **269**: 143-152

24 **Zamzami N**, Hirsch T, Dallaporta B, Petit PX, Kroemer G. Mitochondrial implication in accidental and programmed cell death:apoptosis and necrosis. *J Bioenerg Biomembr* 1997; **29**: 185-193

25 **Brdiczka D**, Beutner G, Rück A, Dolder M, Wallimann T. The molecular structure of mitochondrial contact sites. Their role in regulation of energy metabolism and permeability transition. *Biofactors* 1998; **8**: 235-242

26 **Bopassa JC**, Michel P, Gateau-Roesch O, Ovize M, Ferrera R. Low-pressure reperfusion alters mitochondrial permeability transition. *Am J Physiol Heart Circ Physiol* 2005; **288**: H2750-H2755

27 **Brustovetsky N**, Tropschug M, Heimpel S, Heidkämper D, Klingenberg M. A large Ca^{2+}-dependent channel formed by recombinant ADP/ATP carrier from Neurospora crassa resembles the mitochondrial permeability transition pore. *Biochemistry* 2002; **41**: 11804-11811

28 **Schinzel AC**, Takeuchi O, Huang Z, Fisher JK, Zhou Z, Rubens J, Hetz C, Danial NN, Moskowitz MA, Korsmeyer SJ. Cyclophilin D is a component of mitochondrial permeability transition and mediates neuronal cell death after focal cerebral ischemia. *Proc Natl Acad Sci U S A* 2005; **102**: 12005-12010

29 Kriska T, Korytowski W, Girotti AW. Role of mitochondrial cardiolipin peroxidation in apoptotic photokilling of

5-aminolevulinate-treated tumor cells. *Arch Biochem Biophys* 2005; **433**: 435-446

30 **Hortelano S**, Dallaporta B, Zamzami N, Hirsch T, Susin SA, Marzo I, Boscá L, Kroemer G. Nitric oxide induces apoptosis via triggering mitochondrial permeability transition. *FEBS Lett* 1997; **410**: 373-377

31 **Marchetti P**, Hirsch T, Zamzami N, Castedo M, Decaudin D, Susin SA, Masse B, Kroemer G. Mitochondrial permeability transition triggers lymphocyte apoptosis. *J Immunol* 1996; **157**: 4830-4836

32 **Marchetti P**, Castedo M, Susin SA, Zamzami N, Hirsch T, Macho A, Haeffner A, Hirsch F, Geuskens M, Kroemer G. Mitochondrial permeability transition is a central coordinating event of apoptosis. *J Exp Med* 1996; **184**: 1155-1160

33 **Ning N**, Peng ZF, Yuan L, Gou BD, Zhang TL, Wang K. [Realgar nano-particles induce apoptosis and necrosis in leukemia cell lines K562 and HL-60]. *Zhongguo Zhong Yao Za Zhi* 2005; **30**: 136-140

34 **Ly JD**, Grubb DR, Lawen A. The mitochondrial membrane potential (deltapsi(m)) in apoptosis; an update. *Apoptosis* 2003; **8**: 115-128

35 **Di Lisa F**, Bernardi P. Mitochondrial function and myocardial aging. A critical analysis of the role of permeability transition. *Cardiovasc Res* 2005; **66**: 222-232

S- Editor Wang J **L- Editor** Zhu LH **E- Editor** Liu WF